CHAPTER 13

CONTROL SYSTEM PERFORMANCE MODIFICATION

Suhada Jayasuriya
Department of Mechanical Engineering
Texas A&M University
College Station, Texas

1 INTRODUCTION **503**

2 GAIN AND PHASE MARGIN **504**
2.1 Gain Margin 504
2.2 Phase Margin 504
2.3 Gain-Phase Plots 505
2.4 Polar Plot as a Design Tool in the Frequency Domain 506

3 HALL CHART **509**
3.1 Constant-Magnitude Circles 510
3.2 Constant-Phase Circles 510
3.3 Closed-Loop Frequency Response for Nonunity Feedback Systems 511
3.4 Closed-Loop Amplitude Ratio 512

4 NICHOLS CHART **513**
4.1 Closed-Loop Frequency Response from That of Open Loop 514
4.2 Sensitivity Analysis Using the Nichols Chart 516

5 ROOT LOCUS **517**
5.1 Angle and Magnitude Conditions 518
5.2 Time-Domain Design Using the Root Locus 523
5.3 Time-Domain Response versus *s*-Domain Pole Locations 531

6 POLE LOCATIONS IN THE *z*-DOMAIN **532**
6.1 Stability Analysis of Closed-Loop Systems in the *z*-Domain 535
6.2 Performance Related to Proximity of Closed-Loop Poles to the Unit Circle 536
6.3 Root Locus in the *z*-Domain 537

7 CONTROLLER DESIGN **538**

REFERENCES **540**

BIBLIOGRAPHY **540**

1 INTRODUCTION

Chapter 12 presents a wide variety of tools for analyzing closed-loop control systems. This chapter focuses on the development of additional analytical tools for closed-loop control systems, tools aimed at performance modification and improvement. Each successive tool presented in this chapter is useful in its ability to predict system performance and to pinpoint the appropriate modifications so that the closed-loop system will meet its required performance objectives.

Chapter 14 also addresses the problem of system modifications, but there the emphasis is to work with the adjustable parameters of a device called the servocontroller to achieve the necessary result.

Reprinted from *Instrumentation and Control,* Wiley, New York, 1990, by permission of the publisher.

2 GAIN AND PHASE MARGIN

The Nyquist stability criterion may be conveniently used to define certain measures of relative stability or robustness. We note that the $(-1,0)$ point in the GH plane plays a crucial role in determining the closed-loop stability of a system. If a system's stability status is known, one might be interested in knowing how stable the system is due to changes in parameters. For example, if the system remains stable despite large changes in parameters, then it is said to possess a high degree of relative stability or robustness. Gain margin and phase margin are two measures typically employed to characterize this robustness. They characterize how close the Nyquist plot is to encircling the $(-1,0)$ point in the GH plane.

2.1 Gain Margin

This is a measure of how much the loop gain can be raised before closed-loop instability results. The basic definition of gain margin (GM) is apparent from Fig. 1.

2.2 Phase Margin

The phase margin (PM) is the difference between the phase of $GH(j\omega)$ and 180° when the $GH(j\omega)$ crosses the circle with unit magnitude. A positive PM corresponds to a case where the Nyquist locus does not encircle the $(-1,0)$ point. This is shown in Fig. 2.

A stable system corresponds to gain and phase margins that are positive. In some cases, however, the PM and GM notions break down. For first- and second-order systems, the phase never crosses the 180° line; hence the GM is always ∞. For higher order systems, it is possible to have more than one crossing of the unit amplitude circle and more than one crossing of the 180° line. In such situations the GM and PM are somewhat misleading. Furthermore, non-minimum-phase systems exhibit stability criteria that are opposite to those previously defined.

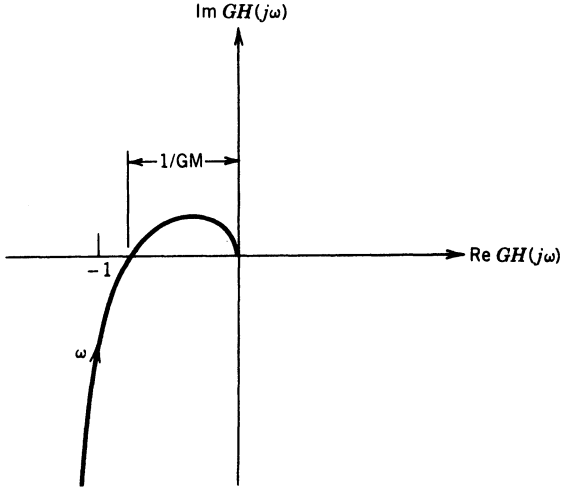


Figure 1 Gain margin.

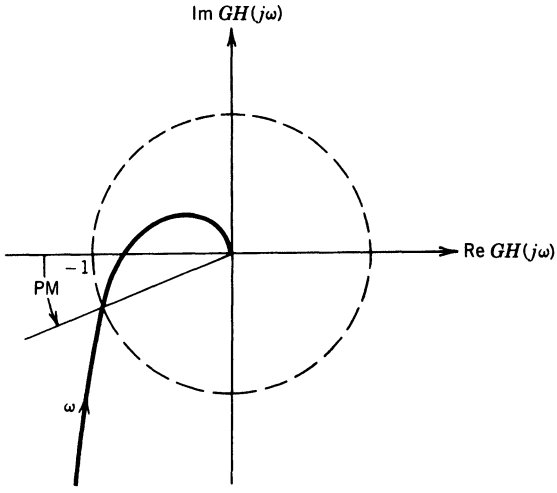


Figure 2 Phase margin.

2.3 Gain-Phase Plots

The graphical representation of the frequency response of the system $G(s)$ using either

$$G(j\omega) = G(s)|_{s=j\omega} = \text{Re } G(j\omega) + j \text{ Im } G(j\omega)$$

or

$$G(j\omega) = |G(j\omega)|e^{j\phi(\omega)}$$

where

$$\phi(\omega) = \underline{/G(j\omega)}$$

is known as the polar plot. The coordinates of the polar plot are the real and imaginary parts of $G(j\omega)$, as shown in Fig. 3.

Example 1 Obtain the polar plot of the transfer function

$$G(s) = \frac{K}{s(\tau s + 1)}$$

The frequency response is given by

$$G(j\omega) = \frac{K}{j\omega(j\tau\omega + 1)}$$

Then the magnitude and the phase can be written as

$$|G(j\omega)| = \frac{K}{\omega\sqrt{\omega^2\tau^2 + 1}}$$

and

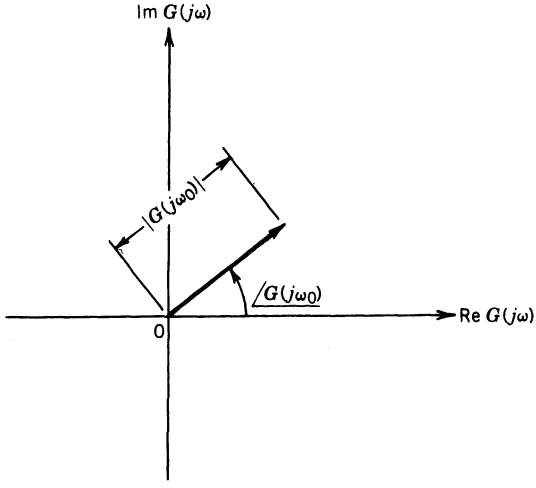


Figure 3 Polar representation.

$$G(j\omega) = -\frac{\pi}{2} - \tan^{-1}\omega\tau$$

If $|G(j\omega)|$ and $\angle G(j\omega)$ are computed for different frequencies, an accurate plot can be obtained. A quick idea can, however, be gained by simply doing a limiting analysis at $\omega = 0$, $\omega = \infty$, and the corner frequency $\omega = 1/\tau$.

We note that

$$|G(j\omega)| \to \infty \qquad \angle G(j\omega) = \frac{-\pi}{2} \qquad \text{for } \omega = 0$$

$$|G(j\omega)| \to 0 \qquad \angle G(j\omega) = -\pi \qquad \text{for } \omega = \infty$$

$$|G(j\omega)| = \frac{K\tau}{\sqrt{2}} \qquad \angle G(j\omega) = -\frac{3\pi}{4} \qquad \text{for } \omega = \frac{1}{\tau}$$

The polar plot is shown in Fig. 4.

A gain-phase plot is where the frequency response information is given with respect to a Cartesian frame with vertical axis for gain and horizontal axis for phase.

2.4 Polar Plot as a Design Tool in the Frequency Domain

As a design tool its best use is in determining relative stability with respect to GM and PM. If the uncertainty in the transfer function can be characterized by bounds on the gain-phase plot, then it allows one to determine what type of compensation needs to be provided for the system to perform in the presence of such uncertainties. As an example consider the closed-loop system shown in Fig. 5.

Suppose the gain-phase plot is known to lie in the shaded region in the $G(j\omega)$ plane, as shown in Fig. 6.

Since the shaded region includes the $(-1,0)$ point, and the true gain-phase plot for the plant can lie anywhere in the shaded region, the system can potentially be unstable. If

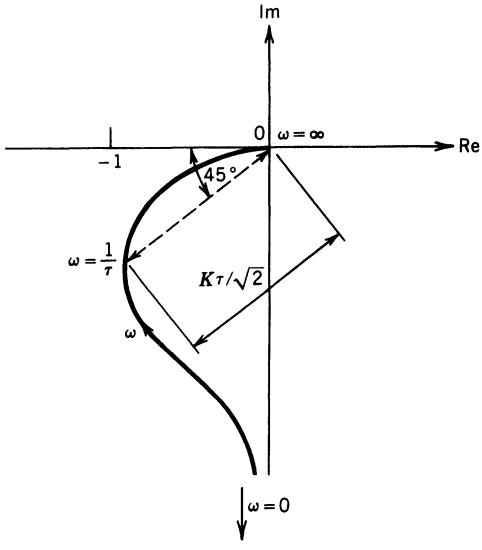


Figure 4 Polar plot for $G(s) = K/s(\tau s + 1)$.

stabilization in the presence of uncertainty is the primary design issue, then we would require a $G_c(s)$ so that it would reshape the high-frequency part of the polar plot with a reduced band of uncertainty. The reduction in the band of uncertainty is a required feature of any sound feedback system design. Qualitatively one would expect to reshape the polar plot to something that looks like what is shown in Fig. 6*b*. Moreover, knowing the important frequency ranges will allow one to be more concerned with relevant portions of the gain-phase plot for reshaping. To further illustrate the basic philosophy of a typical design in the frequency domain, consider the plant transfer function

$$G_p(s) = \frac{K}{s(1 + s)(1 + 0.0125s)}$$

in the feedback configuration shown in Fig. 7.

It is required that when a ramp input is applied to the closed-loop system, the steady-state error of the system does not exceed 1% of the amplitude of the input ramp. Using steady-state error computations we find that the minimum K should be such that

$$\text{Steady-state error} = e_{ss} = \lim_{s \to 0} \frac{1}{sG_p(s)} = \frac{1}{K} \leq 0.01$$

that is, $K \geq 100$.

It can be easily verified that with $G_c(s) = 1$ the system is unstable for $K > 81$, implying that a controller $G_c(s)$ must be designed to satisfy the steady-state performance and relative stability requirements. Putting it another way, the controller must be able to keep the zero-

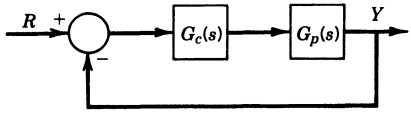


Figure 5 Closed-loop system.

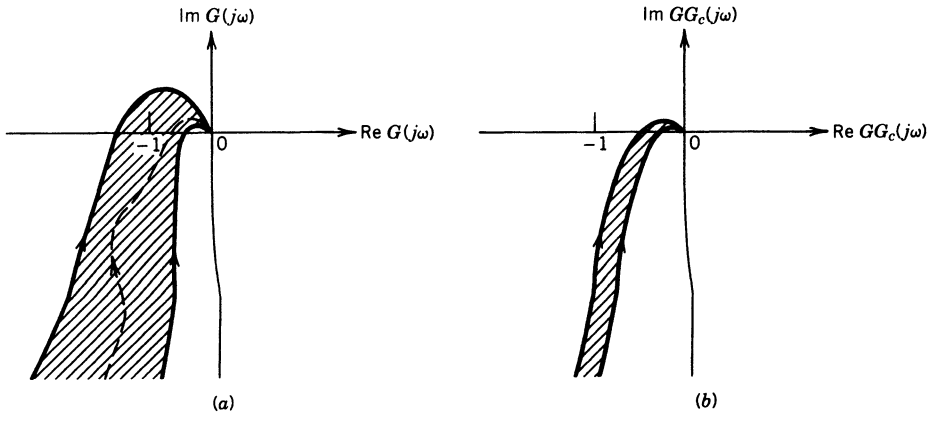


Figure 6 Polar plots for an uncertain system.

frequency gain of $sG_pG_c(s)$ effectively at 100 while maintaining a prescribed degree of relative stability. The principle of the design in the frequency domain is best illustrated by the polar plot of $G_p(s)$ shown in Fig. 8. In practice, the Bode diagram is preferred for design purposes because it is simpler to construct. The polar plot is used mainly for analysis and added insight.

As shown in Fig. 8, when $K = 100$, the polar plot of $G_p(s)$ encloses the $(-1,0)$ point, and the closed-loop system is unstable. Let us assume that we wish to realize that PM = 30°. This means that the polar plot must pass through point A (with magnitude 1 and phase −150°). If K is the only adjustable parameter to achieve this PM, the desired value $K \simeq 3.4$, as shown in Fig. 8. But, K cannot be set to 3.4 since the ramp error constant would only be 3.4 s^{-1}, and the steady-state error requirement will not be satisfied.

Since the steady-state performance of the system is governed by the characteristics of the transfer function at low frequency, and the damping or the transient behavior of the system is governed by the relatively high-frequency characteristics, as Fig. 8 shows, to simultaneously satisfy the transient and the steady-state requirements, the frequency locus of $G_p(s)$ has to be reshaped so that the high-frequency portion of the plot follows the $K = 3.4$ trajectory and the low-frequency portion follows the $K = 100$ trajectory. The significance of this reshaping of the frequency locus is that the compensated locus shown in Fig. 8 will be coincident with the high-frequency portion yielding PM = 30°, while the zero-frequency gain is maintained at 100 to satisfy the steady state requirement.

When we inspect the loci of Fig. 8, we see that there are at least two alternatives in arriving at the compensated locus:

1. Starting from the $K = 100$ locus and reshaping the locus in the region near the gain crossover frequency ω_g while keeping the low-frequency region of $G_p(s)$ relatively unaltered

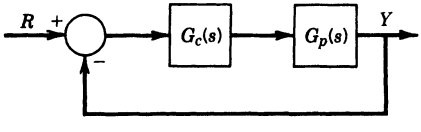


Figure 7 Closed-loop system with $G(s) = K/[s(s + 1)(0.0125s + 1)]$.

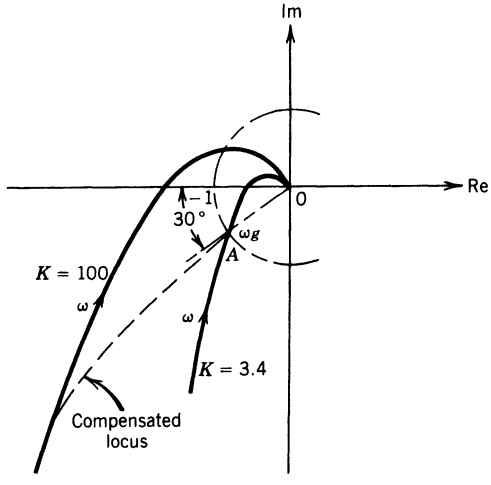


Figure 8 Polar plot for open-loop system transfer function of Fig. 7.

2. Starting from the $K = 3.4$ locus and reshaping the low-frequency portion of $G_p(s)$ to obtain an error constant of 100 while keeping the locus near $\omega = \omega_g$ relatively unchanged

In the first approach, the high-frequency portion of $G_p(s)$ is pushed in the counterclockwise (CCW) direction, which means that more phase is added to the system in the positive direction in the proper frequency range. This scheme is basically phase-lead compensation and controllers used for this purpose are often of the high-pass filter type. The second approach apparently involves the shifting of the low-frequency part of the $K = 3.4$ trajectory in the clockwise (CW) direction, or alternatively reducing the magnitude of $G_p(s)$ with $K = 100$ at the high-frequency range. This scheme is often referred to as phase-lag compensation since more phase lag is introduced to the system in the low-frequency range. The controllers used for this purpose are often referred to as low-pass filters.

3 HALL CHART

In typical frequency response design only the open-loop transfer function is plotted. Therefore it is useful to know how the closed-loop performance is related to the open loop. Hall charts provide a convenient way of carrying out a frequency response design with closed-loop performance specifications. One important consideration is the maximum closed-loop gain. Another is the closed-loop phase. A Hall chart primarily consists of constant closed-loop gain loci and constant closed-loop phase loci. A design would then proceed by drawing the open-loop polar plot on the Hall chart.

For a unity negative-feedback system as shown in Fig. 9 the closed-loop transfer function is

$$\frac{C(s)}{R(s)} = \frac{G(s)}{1 + G(s)} \tag{1}$$

In the following discussion we assume that the polar plot of $G(j\omega)$ is known.

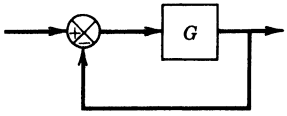


Figure 9 Unity negative-feedback system.

3.1 Constant-Magnitude Circles

The loci on which the closed-loop magnitude

$$\left|\frac{C(s)}{R(s)}\right| = \left|\frac{G(s)}{1 + G(s)}\right| = M = \text{const}$$

are referred to as constant-magnitude loci. In fact these loci are circles in the $G(j\omega)$-plane. This can be established by noting a typical point on the $G(j\omega)$ plot as $X + jY$.

Then

$$M = \frac{|X + jY|}{|1 + X + jY|}$$

and

$$M^2 = \frac{X^2 + Y^2}{(1 + X)^2 + Y^2}$$

Hence

$$X^2 + \frac{2M^2}{M^2 - 1} X + \frac{M^2}{M^2 - 1} + Y^2 = 0$$

which can be written as

$$\left(X + \frac{M^2}{M^2 - 1}\right)^2 + Y^2 = \frac{M^2}{(M^2 - 1)^2} \tag{2}$$

Equation (2) is the equation of a circle with center at $X = -M^2/(M^2 - 1)$, $Y = 0$ and with radius $|M/(M^2 - 1)|$. A family of constant-M circles is shown in Fig. 10. Given a point $P \equiv (X_1, Y_1)$ on an open-loop polar plot $G(j\omega)$, the corresponding closed-loop magnitude can be determined by locating the M circle passing through that point.

Graphically the intersection of the $G(j\omega)$ plot and the constant-M locus gives the value of M at the frequency denoted on the $G(j\omega)$ curve. If it is desired to keep the value of the maximum closed-loop gain M_r less than a certain value, the $G(j\omega)$ curve must not intersect the corresponding M circle at any point and at the same time must not enclose the $(-1,j0)$ point. The constant-M circle with the smallest radius that is tangent to the $G(j\omega)$ curve gives the value of M_r, and the resonant frequency ω_r is read off at the tangent point on the $G(j\omega)$ curve.

3.2 Constant-Phase Circles

The loci of constant phase of the closed-loop system can also be determined in the $G(j\omega)$-plane by a method similar to that used for constant-M loci. With reference to Eq. (1) the phase of the closed-loop system corresponding to the point $P = X + jY$ is written as

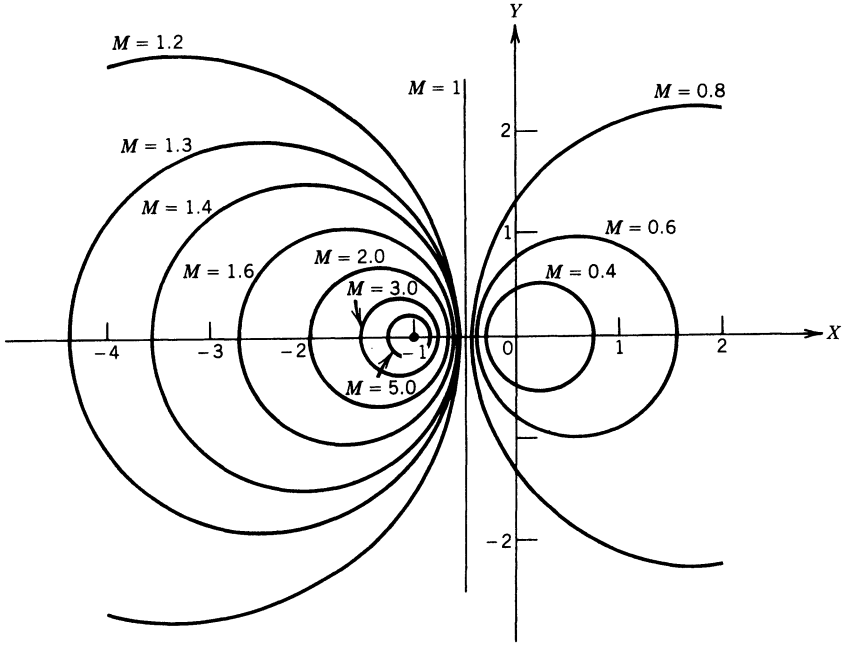


Figure 10 Family of constant-M circles.

$$\phi = \tan^1\left(\frac{Y}{X}\right) - \tan^1\left(\frac{Y}{1+X}\right) \tag{3}$$

Taking the tangent on both sides of Eq. (3) and rearranging yields

$$\left(X + \frac{1}{2}\right)^2 + \left(Y - \frac{1}{2N}\right)^2 = \frac{1}{4} + \left(\frac{1}{2N}\right)^2 \tag{4}$$

where $N = \tan \phi$.

Equation (4) represents a family of circles with center at $(-1/2, 1/2N)$ and with radius $\sqrt{1/4 + 1/(2N)^2}$. The constant-phase loci are shown in Fig. 11.

The use of constant-magnitude and constant-phase circles enables one to find the entire closed-loop frequency response from the open-loop frequency response $G(j\omega)$ without calculating the magnitude and phase of the closed-loop transfer function at each frequency. The intersections of the $G(j\omega)$ locus and the M circles and N circles give the values of M and N at frequency points on the $G(j\omega)$ locus.

3.3 Closed-Loop Frequency Response for Nonunity Feedback Systems

The constant-M and constant-N circles are limited to closed-loop systems with unity negative feedback, whose transfer function is given by Eq. (1). When a system has nonunity feedback, the closed-loop transfer function is

$$\frac{C(s)}{R(s)} = \frac{G(s)}{1 + G(s)H(s)} \tag{5}$$

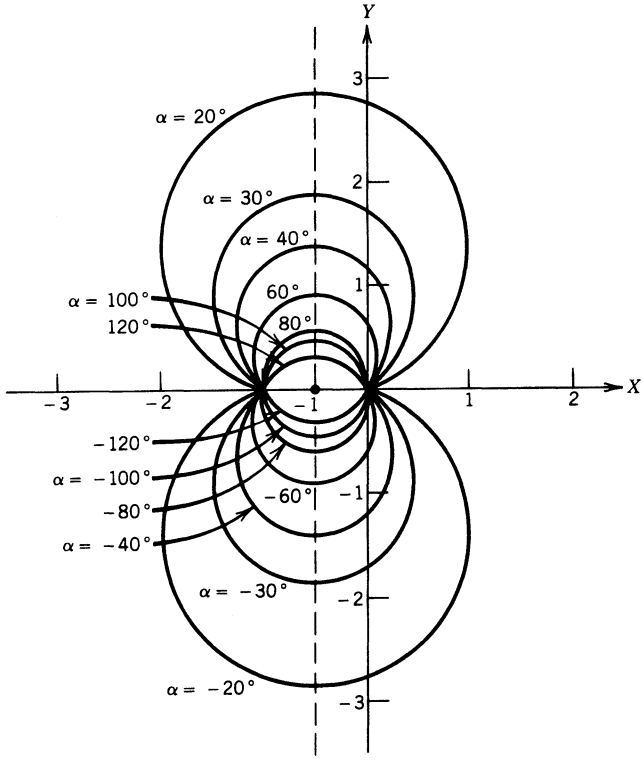


Figure 11 Family of constant-N circles.

and constant-M loci derived earlier cannot be directly applied. However, with a slight modification constant-M and constant-N loci can still be applied to systems with nonunity feedback. We modify Eq. (5) as

$$\frac{C(s)}{R(s)} = \frac{1}{H(s)} \frac{G(s)H(s)}{1 + G(s)H(s)}$$

The magnitude and phase angle of $G_1(s)/[1 + G_1(s)]$, where $G_1(s) = G(s)H(s)$, may be obtained easily by plotting the $G_1(j\omega)$ locus and reading the values of M and N at various frequency points. The closed-loop frequency response $C(j\omega)/R(j\omega)$ may then be obtained by multiplying $G_1(j\omega)/[1 + G_1(j\omega)]$ by $1/H(j\omega)$.

3.4 Closed-Loop Amplitude Ratio

In obtaining suitable performance, the adjustment of gain is usually the first consideration. The adjustment of gain is usually based on the maximum closed-loop gain or the resonant peak. That is the gain K which must be chosen so that over the entire frequency range the closed-loop amplitude ratio M_r is not exceeded.

Consider first isolating the circle corresponding to M_r as shown in Fig. 12. Then a tangent line to the M_r circle is drawn from the origin, which makes an angle ψ with the real line.

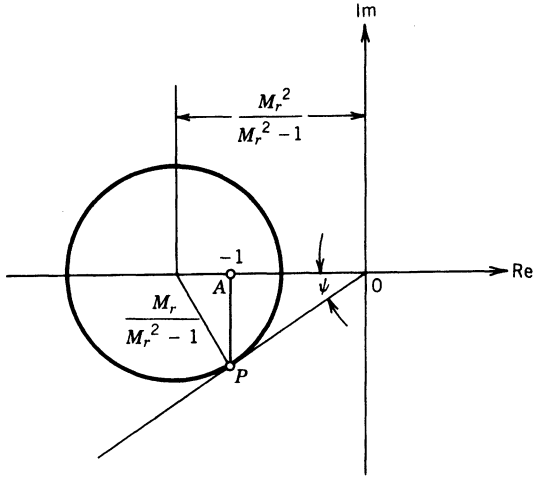


Figure 12 *M* circle.

If $M_r > 1$, then

$$\sin \psi = \left| \frac{M_r/(M_r^2 - 1)}{M_r^2/(M_r^2 - 1)} \right| = \frac{1}{M_r}$$

It can be shown that the line drawn from P perpendicular to the negative real axis intersects this axis at the $(-1,0)$ point. These two facts, namely $\sin \psi = 1/M_r$ and that the normal from P passes through $(-1,0)$, can be used to determine the appropriate gain K.

Example 2 Consider the system shown in Fig. 13*a*: Determine K so that $M_r = 1.4$. First sketch the polar plot of

$$\frac{G(j\omega)}{K} = \frac{1}{j\omega(1 + j\omega)}$$

as shown in Fig. 13*b*. The value of ψ corresponding to $M_r = 1.4$ is obtained from

$$\psi = \sin^{-1} \frac{1}{M_r} = \sin^{-1} \frac{1}{1.4} = 45.6°$$

The next step is to draw a line OP that makes an angle $\psi = 45.6°$ with the negative real axis. Then draw the circle that is tangent to both the $G(j\omega)/K$ locus and the line OP. The perpendicular line drawn from the point P intersects the negative real axis at $(-0.63,0)$. Then the gain K of the system is determined as follows:

$$K = \frac{1}{0.63} = 1.58$$

4 NICHOLS CHART

Both the gain and phase plots are generally required to analyze the performance of a closed-loop system. A major disadvantage in working with polar plots is that the curve no longer

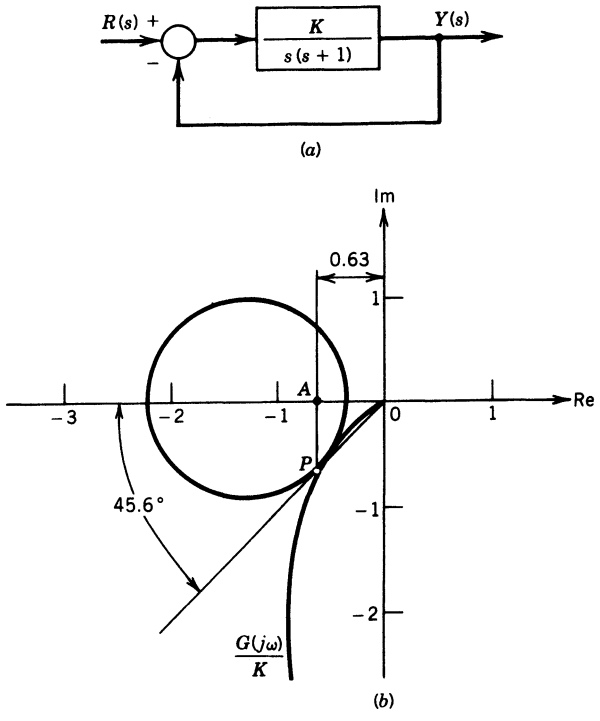


Figure 13 (*a*) Closed-loop system; (*b*) determination of the gain K using an M circle.

retains its original shape when a simple modification such as the change of the loop gain is made to the system. In design, however, not only the loop gain must be altered but often series or feedback controllers are to be added to the original system that require the complete reconstruction of the resulting open-loop transfer function. For design purposes it is more convenient to work with Bode diagrams or gain-versus-phase plots. The latter representation with corresponding M and N circles superimposed on it is referred to as the *Nichols chart.* In a gain-versus-phase plot the entire $G(j\omega)$ is shifted up or down vertically when the gain is altered. A Nichols chart is shown in Fig. 14.

This chart is symmetric about the $-180°$ axis. The M and N loci repeat for every 360°, and there is symmetry at every 180° interval. The M loci are centered about the critical point (0 dB, −l80°).

4.1 Closed-Loop Frequency Response from That of Open Loop

It is quite easy to determine the closed-loop frequency response from that of the open loop by using the Nichols chart. If the open-loop frequency response curve is superimposed on the Nichols chart, the intersections of the open-loop frequency response curve $G(j\omega)$ and the M and N loci give the magnitude M and phase angle ϕ of the closed-loop frequency response at each frequency point. If the $G(j\omega)$ locus does not intersect the $M = M_r$ locus but is tangent to it, then the resonant peak value of the closed-loop frequency response is given by M_r. The resonant frequency is given by the frequency at the point of tangency.

As an example consider the unity negative-feedback system with the following open-loop transfer function:

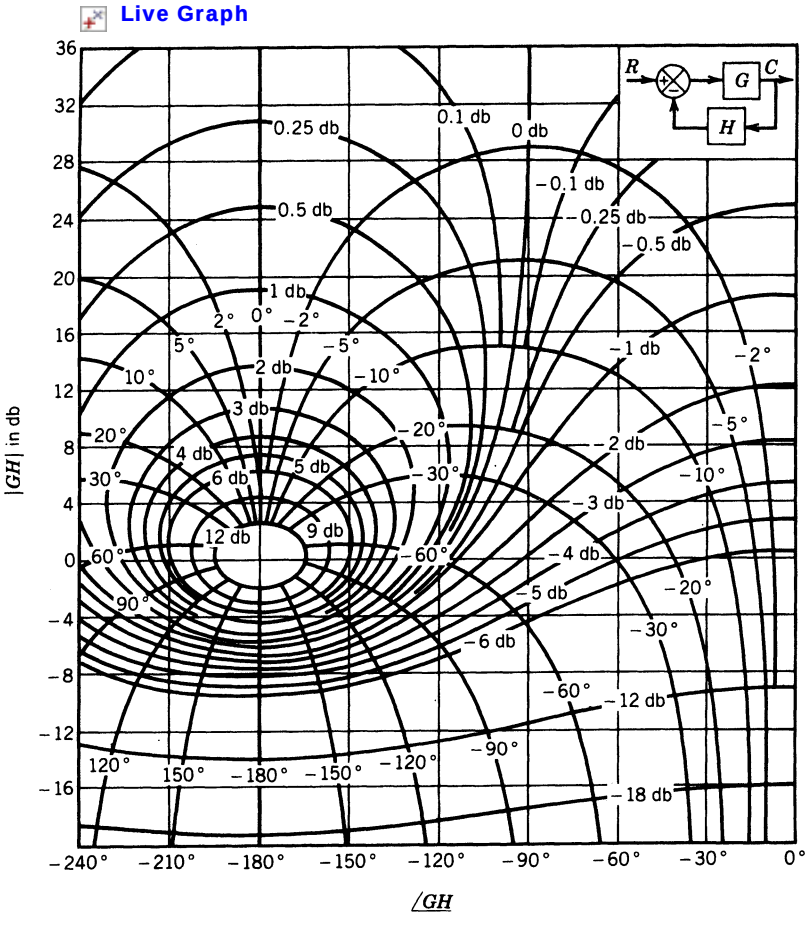


Figure 14 Nichols chart.

$$G(s) = \frac{K}{s(s+1)(0.5s+1)} \qquad K = 1$$

To find the closed-loop frequency response by use of the Nichols chart, the $G(j\omega)$ locus is first constructed. (It is easy to first construct the Bode diagram and then transfer values to the Nichols chart.) The closed-loop frequency response curves (gain and phase) may be constructed by reading the magnitude and phase angles at various frequency points on the $G(j\omega)$ locus from the M and N loci as shown in Fig. 15. Since the $G(j\omega)$ locus is tangent to the $M = 5$-dB locus, the peak value of the closed-loop frequency response is $M_r = 5$ dB, and the resonant frequency is 0.8 rad/s.

The bandwidth of the closed-loop system can easily be found from the $G(j\omega)$ locus in the Nichols chart. The frequency at the intersection of the $G(j\omega)$ locus and the $M = -3$-dB locus gives the bandwidth. The gain and phase margins can be read directly from the Nichols chart.

If the open-loop gain K is varied, the shape of the $G(j\omega)$ locus in the Nichols chart remains the same but is shifted up (for increasing K) or down (for decreasing K) along the vertical axis. Therefore the modified $G(j\omega)$ locus intersects the M and N loci differently, resulting in a different closed-loop frequency response curve.

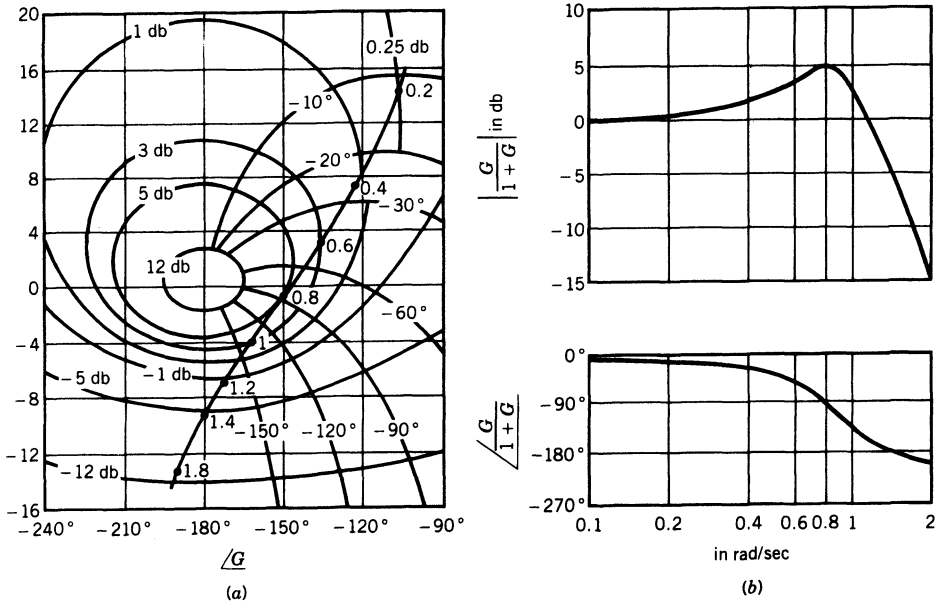


Figure 15 (*a*) Plot of $G(j\omega)$ superimposed on Nichols chart; (*b*) closed-loop frequency response curves.

4.2 Sensitivity Analysis Using the Nichols Chart[1]

Consider a unity feedback system with the transfer function

$$\frac{C(s)}{R(s)} = \frac{G(s)}{1 + G(s)} = G_{\text{cl}}(s)$$

The sensitivity of $G_{\text{cl}}(s)$ with respect to $G(s)$ is defined as

$$S_G^{G_{\text{cl}}}(s) = \frac{dG_{\text{cl}}(s)/G_{\text{cl}}(s)}{dG(s)/G(s)}$$

which yields

$$S_G^{G_{\text{cl}}}(s) = \frac{1}{1 + G(s)} \tag{6}$$

Clearly the sensitivity function is a function of the complex variable s.

To design a system with a prescribed sensitivity, the Nichols chart is quite convenient. Equation (6) is written as

$$S_G^{G_{\text{cl}}}(j\omega) = \frac{G^{-1}(j\omega)}{1 + G^{-1}(j\omega)}$$

which clearly indicates that the magnitude and phase of $S_G^{G_{\text{cl}}}(j\omega)$ can be obtained by plotting $G^{-1}(j\omega)$ on the Nichols chart and making use of the constant-M loci for a constant sensitivity function. Since the vertical coordinate of the Nichols chart is in decibels, the $G^{-1}(j\omega)$ curve on the Nichols chart can be easily obtained if $G(j\omega)$ is already available since

$$|G^{-1}(j\omega)|_{\text{dB}} = -|G(j\omega)|_{\text{dB}}$$

$$\underline{/G^{-1}(j\omega)} = -\underline{/G(j\omega)}$$

As an example consider the unity feedback system with the open-loop transfer function

$$G(s) = \frac{400{,}000K}{s(s + 49)(s + 991)}$$

the function $G^{-1}(j\omega)$ is plotted on the Nichols chart, as shown in Fig. 16, for $K = 2.94$. The intersections of the $G^{-1}(j\omega)$ curve with the M loci give the magnitude of $S_G^{G_{\text{cl}}}(j\omega)$ at the corresponding frequencies. Figure 16 indicates several interesting points with regard to the sensitivity function of the feedback system. The sensitivity function approaches 0 dB or unity as $\omega \to \infty$: $S_G^{G_{\text{cl}}} \to 0$ as $\omega \to 0$. A peak value of 1.1 dB is reached at $\omega = 25$ rad/s. This means that the closed-loop system is most sensitive to a change of $G(j\omega)$ at this frequency and more generally in this frequency range.

5 ROOT LOCUS

Poles and zero locations of a dynamic system characterize the system performance in a significant way. The root-locus method allows one to investigate the closed-loop pole patterns of a dynamic system with respect to a single parameter.

A typical closed-loop characteristic equation (CLCE) of a feedback system can be written as

$$1 + G(s)H(s) = 0 \tag{7}$$

where $G(s)H(s)$ is the open-loop transfer function.

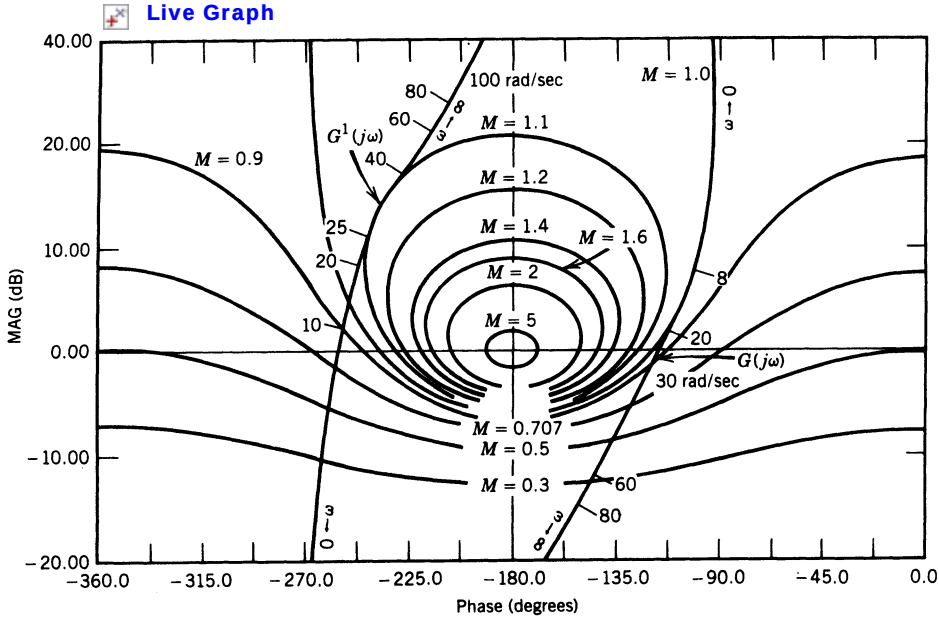


Figure 16 Determination of the sensitivity function S_G^M in the Nichols chart.

If $G(s)H(s)$ has a single parameter K as a variable, then by rewriting as

$$1 + KG(s)H(s) = 0 \tag{8}$$

a standard procedure for obtaining the closed-loop poles corresponding to any K is the Evans root-locus method.

5.1 Angle and Magnitude Conditions

The CLCE [Eq. (8)] can be written as

$$KG(s)H(s) = -1 = e^{j(2\pi l \pm \pi)} \tag{9}$$

Thus, any point s_0 satisfying the condition

$$\underline{/KG(s_0)H(s_0)} = (2l \pm 1)\pi \tag{10}$$

satisfies Eq. (8). If $K > 0$, then Eq. (10) reduces to

$$\underline{/G(s_0)H(s_0)} = (2l \pm 1)\pi \tag{11}$$

and is commonly called the angle condition. All points s_0 in the complex plane satisfying this angle condition satisfy the closed-loop characteristic equation and hence are said to lie on the root locus. If s_0 is a point on the root loci, then the corresponding value of K may be computed by noting that

$$|K||G(s_0)||H(s_0)| = 1 \tag{12}$$

which is called the amplitude condition.

By studying the angle condition in detail of the CLCE,

$$\underline{/1 + KG(s)H(s)} = 1 + K\frac{\prod_{i=1}^{m}(s + z_i)}{\prod_{j=1}^{n}(s + p_j)}$$

a set of rules can be developed for constructing the root locus easily. These rules are given next without proof.[2]

Rule 1. The system root loci have n branches originating at the n open-loop poles $-p_j$, $j = 1, \ldots, n$, with the value $K = 0$.

Rule 2. Out of the n branches m number of branches will terminate on m finite zeros $-z_i$, $i = 1, 2, \ldots, m$, of the open-loop transfer function at $K = \infty$.

Rule 3. The remaining $n - m$ branches will go to ∞ along asymptotes as $K \to \infty$. The asymptotes are straight lines meeting at a point on the real line called the hub with specific orientation as given in rule 4.

Rule 4. *a*. The asymptotes meet at the hub

$$\sigma = \frac{\sum_{j=1}^{n} \text{poles} - \sum_{i=1}^{m} \text{zeros}}{n - m} = \frac{\sum_{j=1}^{n}(-p_j) - \sum_{i=1}^{m}(-z_i)}{n - m}$$

b. The $n - m$ asymptote angles are given by

$$\theta_N = \pm\frac{180°N}{n - m}$$

where N takes on values 1, 3, 5, 7, ... For each N, two angles are computed and the procedure is repeated until $n - m$ angles are obtained.

Rule 5. If to the right of a point on the real axis there lies an odd number of open-loop poles and zeros, then it is a point on the root loci.

Rule 6. If two open-loop poles or two open-loop zeros are connected, then there must be a break point between the two (Fig. 17).

If an open-loop pole $-p_l$ and an open-loop zero $-z_q$ are connected, in most cases it may be considered as a full branch of the root loci, that is, that the closed-loop pole corresponding to the open-loop pole $-p_l$ starts at $-p_l$ for $K = 0$ and reaches the closed-loop pole signified by the open-loop zero $-z_q$ as $K = \infty$.

Note: Exceptions to this rule exist. Some typical situations are depicted in Fig. 18*a*.

To determine the occurrence of such multiple break points, the next rule may be used.

Rule 7. The break points may be computed by determining points for which $dK/ds = 0$:

$$1 + KGH = 0$$

$$-K = \frac{1}{GH} = \frac{B(s)}{A(s)}$$

$$\frac{dK}{ds} = B(s)\frac{dA(s)}{ds} - A(s)\frac{dB(s)}{ds} = 0$$

Break points coupled with information from rule 6 make it rather easy to pin down the branches.

Rule 8. The points at which the branches cross the imaginary axis can be determined by letting $s = j\omega$ in the characteristic equation.

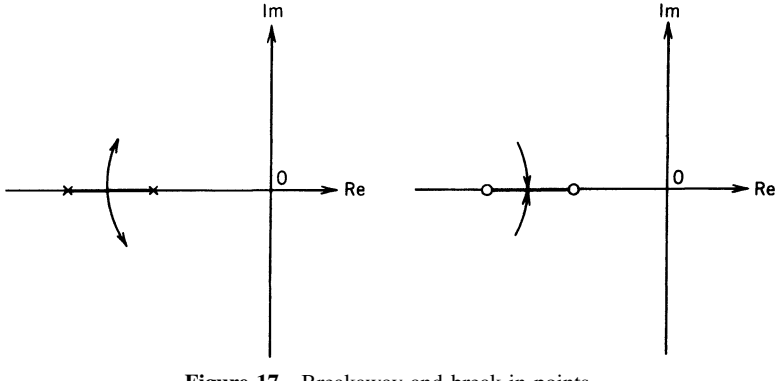


Figure 17 Breakaway and break-in points.

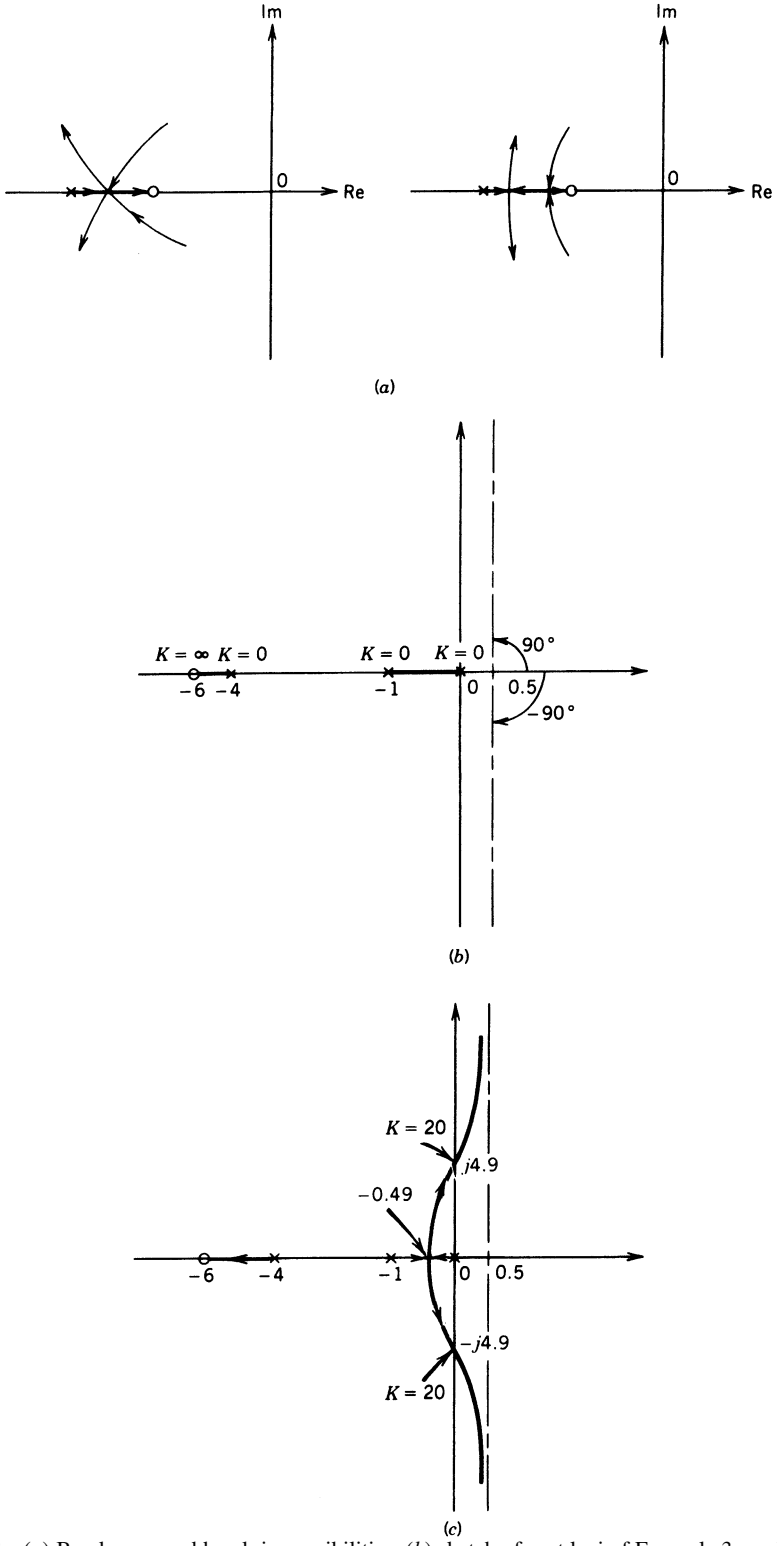


Figure 18 (*a*) Breakaway and break-in possibilities; (*b*) sketch of root loci of Example 3 resulting from rules R1–R4; (*c*) root loci for Example 3 where $G(s) = K(s + 6)/s(s + 1)(s + 4)$.

Rule 9. The angle condition is made use of to determine the angle by which a branch would depart from a pole or would arrive at a zero as $K \to \infty$.

A point s_0 is considered very near the pole (zero) and the angle $G(s_0)H(s_0)$ is computed. The fact that s_0 is very near the pole (zero) makes all but one angle fixed. Thus by employing the angle condition, the unknown angle of departure (arrival) can be computed.

An example is given next to illustrate the various rules for constructing a root locus.

Example 3 Consider CLCE

$$1 + KG(s)H(s) = 1 + \frac{K(s + 6)}{s(s + 1)(s + 4)}$$

R1: $n = 3 \Rightarrow 3$ branches originating at $0, -1, -4$ at $K = 0$.

R2: $m = 1 \Rightarrow 1$ branch terminates at -6, at $K\ \infty$.

R3: $n - m = 2$ branches approach ∞ along asymptotes.

R4: Hub $\sigma = (0 - 1 - 4 - (-6))/2 = 0.5$.

$$\text{Asymptote angles:} \qquad \pm\frac{180^\circ N}{n - m} = \pm\frac{180^\circ N}{2}$$

$$\text{Set } N = 1 \Rightarrow \pm\ 90^\circ$$

R1–R4: Yield the sketch of Fig. 18*b*.

R5: Sections on the real line are 0 to -1 and -4 to -6.

R6: There must be a breakaway point between 0 and -1.

R7: Break points $dK/ds = 0$.

$$\Rightarrow (s + 6)(3s^2 + 10s + 4) - (s^3 + 5s^2 + 4s) = 0$$

$$s^3 + 11.5s^2 + 30s + 12 = 0$$

$$(s + 0.49)(s + 7.89)(s + 3.12) = 0$$

Values for s of -7.89 and -3.12 are unacceptable from R5. Therefore the only breakaway point is at -0.49. A sketch of the root loci is given in Fig. 18*c*.

R8: Imaginary axis crossings:

$$\text{CLCE} = s^3 + 5s^2 + (4 + K)s + 6K = 0$$

Now lets $s = j\omega$:

$$(j\omega)^3 + 5(j\omega)^2 + (4 + K)j\omega + 6K = 0$$

$$(6k - 5\omega^2) + j\omega[(4 + K) - \omega^2] = 0$$

Therefore

$$6K = 5\omega^2$$

$$\omega[4 + K - \omega^2] = 0$$

yielding

$$K = 0 \qquad \omega = 0$$

and

$$K = 20 \qquad \omega = \pm 4.9$$

Example 4 Consider the unity negative-feedback system shown in Fig. 19*a*. Obtain the loci of the closed-loop poles as α is varied from 0 to ∞, that is, obtain the root loci for $0 \leq \alpha \leq \infty$.

Solution: The root loci are the points s satisfying the CLCE:

$$1 + \frac{750}{(s + 5)(s + 10)(s + \alpha)} = 0$$

To utilize the rules for constructing the root loci, the CLCE is rearranged in the form of Eq. (8).

By expanding and rearranging, we get

$$\text{CLCE} = s(s + 5)(s + 10) + \alpha(s + 5)(s + 10) + 750 = 0$$

or

$$1 + \frac{\alpha(s + 5)(s + 10)}{(s + 15)(s^2 + 50)} = 0 \tag{13}$$

Equation (13) has three poles at -15, $+j\sqrt{50}$, $-j\sqrt{50}$ and two finite zeros at -5, -10.

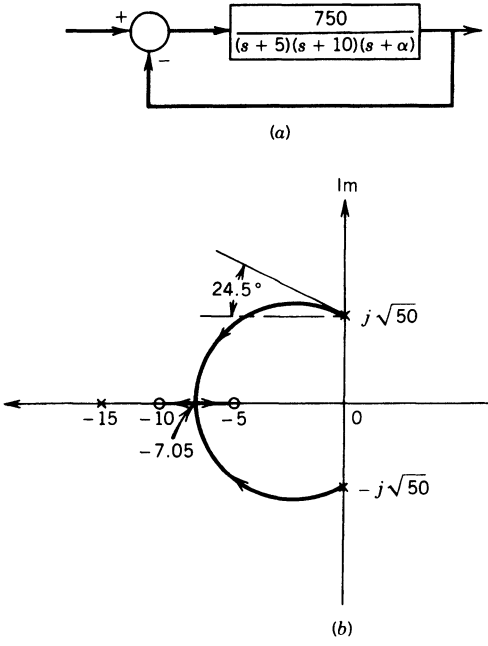


Figure 19 (*a*) Closed-loop system of Example 4; (*b*) root loci of system of Example 4 where $G(s) = \alpha(s + 5)(s + 10)/(s + 15)(s + 50)$.

R1: $n = 3$ implies there are three branches originating at -15, $+j\sqrt{50}$, $+j\sqrt{50}$ at $K = 0$.

R2: $m = 2$ implies two of the three branches terminate on -5, -10 at $K = \infty$.

R3: $n - m = 1$ implies that there is one asymptote.

R4: For a single asymptote a hub does not exist,

$$\text{Asymptote angle} = \pm\frac{180^\circ \text{ N}}{n - m} = \pm\frac{180^\circ \text{ N}}{1}$$

that is, $\theta_1 = 180^\circ$

R5: There is a section of the root loci between $-\infty$ and -15 and between -10 and -5.

R6: Since the two zeros -5 and -10 are connected, there must be a break-in point between -5 and -10. The section -15 to $-\infty$ forms a full branch.

R7: Break points: Since

$$G(s)H(s) = \frac{A(s)}{B(s)} = \frac{s^2 + 15s + 50}{s^3 + 15s^2 + 50s + 750}$$

$$\frac{d\alpha}{ds} = (s^2 + 15s + 50)(3s^2 + 30s + 50) - (s^3 + 15s^2 + 50s + 750)(2s + 15) = 0$$

that is,

$$s^4 + 30s^3 - 85s^2 - 8750 = 0 \tag{14}$$

Thus $s = -7.05$ is a break point.

Remark

To obtain the break points, the fourth-order polynomial in s given in (14) must be factored. However, knowing that there must be a break point in the range -5 and -10 (rule 6), it is quite easy to find the breakaway point. If all roots of (14) are found anyway, then only those points yielding $\alpha \leq 0$ are admissible as break points.

For this example R1–R6 give all the essential information to sketch the root loci of Fig. 19*b*. If the angles of departure are needed, we can employ rule 9.

Consider the point s_0 closer to $+j\sqrt{50}$ and write down the angle condition:

$$\underline{/(s_0 + 5)} + \underline{/(s_0 + 10)} - \underline{/(s_0 + 15)} - \underline{/(s_0 + j\sqrt{50})} - \underline{/(s_0 - j\sqrt{50})} = \pi$$

Now let $s_0 \to j\sqrt{50}$ to yield

$$\underline{/(5 + j\sqrt{50})} + \underline{/(10 + j\sqrt{50})} - \underline{/(15 + j\sqrt{50} - j2\sqrt{50})} - \theta = \pi$$

$$\tan^{-1}\frac{\sqrt{50}}{5} + \tan^{-1}\frac{\sqrt{50}}{10} - \tan^{-1}\frac{\sqrt{50}}{15} - \frac{\pi}{2} - \theta = \pi$$

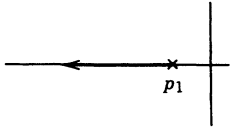
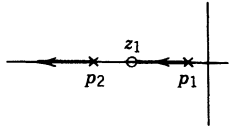
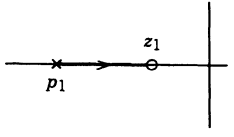
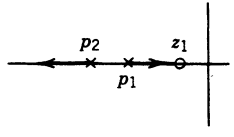
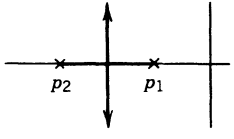
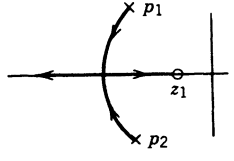
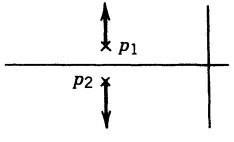
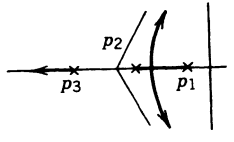
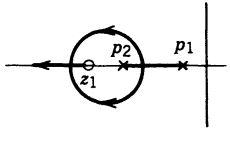
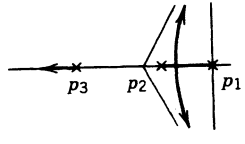
$$\theta = -3.57 \text{ rad} = -204.5^\circ$$

Some typical root-loci plots are shown in Table 1.

5.2 Time-Domain Design Using the Root Locus

Time-domain performance specifications can often be related in an approximate sense to closed-loop pole locations. If suitable pole locations for a certain time-domain performance can be effectively identified, then the root loci can be used to locate the closed-loop poles

Table 1 Typical Root-Loci Plots

No.	$G_0(s)$	Root Loci	No.	$G_0(s)$	Root Loci
1	$\frac{1}{s - p_1}$		6	Same as 5 $p_2 < z_1 < p_1$	
2	$\frac{s - z_1}{s - p_1}$		7	Same as 5 $p_1, p_2 < z_1$	
3	$\frac{1}{(s - p_1)(s - p_2)}$		8	Same as 5 p_1, p_2 complex	
4	$\frac{1}{(s - p_1)(s - p_2)}$ p_1, p_2 complex		9	$\frac{1}{(s - p_1)(s - p_2)(s - p_3)}$	
5	$\frac{(s - z_1)}{(s - p_1)(s - p_2)}$ $z_1 < p_1, p_2$		10	$\frac{1}{s(s - p_2)(s - p_3)}$	

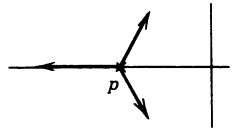
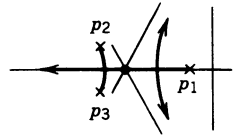
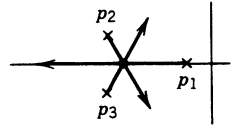
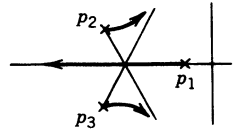
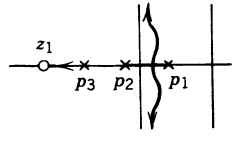
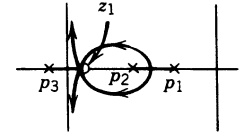
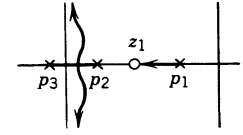
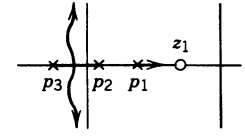
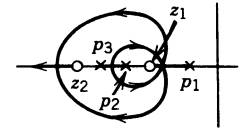
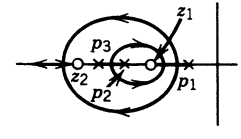
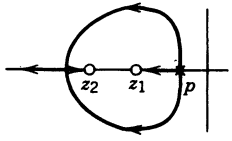
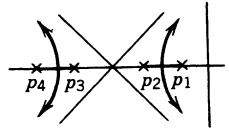
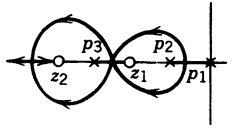
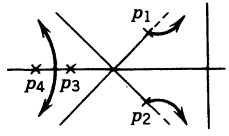
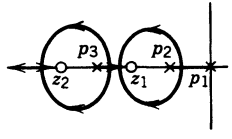
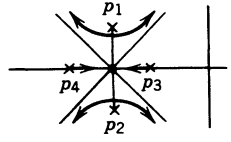
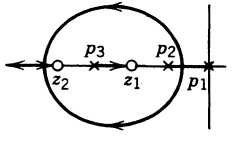
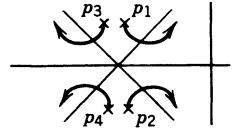
11	$\dfrac{1}{(s-p)^3}$	
12	$\dfrac{1}{(s-p_1)(s-p_2)(s-p_3)}$ p_2, p_3 complex	
13	Same as 12	
14	Same as 12	
15	$\dfrac{(s-z_1)}{(s-p_1)(s-p_2)(s-p_3)}$	
16	Same as 15	
17	Same as 15	
18	Sams as 15	
19	$\dfrac{(s-z_1)(s-z_2)}{(s-p_1)(s-p_2)(s-p_3)}$	
20	Same as 19	

Table 1 (*Continued*)

No.	$G_0(s)$	Root Loci	No.	$G_0(s)$	Root Loci
21	$\dfrac{(s-z_1)(s-z_2)}{(s-p)^3}$ $z_2 < z_1 < p$		25	$\dfrac{1}{(s-p_1)(s-p_2)(s-p_3)(s-p_4)}$ All poles real	
22	$\dfrac{(s-z_1)(s-z_2)}{s(s-p_2)(s-p_3)}$ $z_2 < p_3 < z_1 < p_2 < 0$		26	Same as 25 Two poles real, two poles complex	
23	Same as 22		27	Same as 26	
24	Same as 22		28	Same as 25 All poles complex	

at those locations by appropriate compensation. Compensation can be provided by introducing additional dynamics into the feedback system in the form of increased poles and zeros [proportional-integral-derivative (PID) control, lead, lag, lead–lag, etc.]. We shall now consider some examples to illustrate this time-domain design philosophy.

Example 5 Obtain the root loci for a system with an open-loop transfer function

$$G(s) = \frac{K}{s(s + 2)}$$

(a) Indicate the location of closed-loop poles when $K = 4$ and determine the damping ratio ζ and the natural frequency ω_n corresponding to $K = 4$.

(b) It is now required to double the natural frequency while keeping the same damping ratio. Design a compensator for satisfying the new design specifications.

Solution: (a) Suppose the closed-loop system is as shown in Fig. 20*a*. Then its root loci are as shown in Fig. 20*b*. To find the poles at $K = 4$, solve the CLCE

$$1 + \frac{4}{s(s + 2)} = 0 \qquad \text{or} \qquad s^2 + 2s + 4 = 0$$

The roots are $s_{1,2} = -1 \pm j\sqrt{3}$.

$$\zeta = \cos \beta = 0.5$$

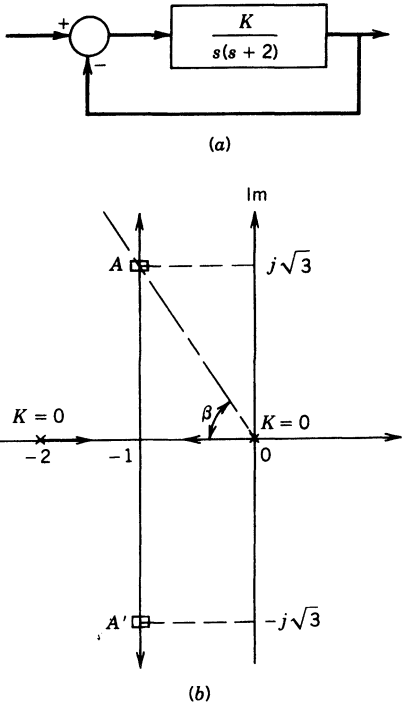


Figure 20 (*a*) Time-domain design example; (*b*) sketch of root loci.

(b) Since the natural frequency is to be doubled keeping the same damping ratio, we need to move the closed-loop poles at A and A' in Fig. 21 so that $\overline{OB} = 2\overline{OA}$.

To satisfy the design specifications, the modified root loci must be made to pass through B and B'. To reshape the original root loci, additional poles and zeros are required. We give below a simple way to appropriately modify the root loci. Conceptually, the modification takes place as shown in Fig. 22.

If $G_c(s)$ is chosen to cancel the pole at -2 by selecting

$$G_c(s) = \frac{s + 2}{s + p}$$

then we only need to find p so that the modified root locus passes through B. This is quite easy to do by noting that the pole–zero cancellation at -2 leaves us with a second-order system with the two open-loop poles at 0 and $-p$.

By selecting $p = +4$, it is easy to verify that the modified root loci are as shown in Fig. 22. So the compensator

$$G_c(s) = \frac{s + 2}{s + 4}$$

will work.

Remark

Pole–zero cancellation as was done here must be avoided if it lies in the right-half plane. Since any real system model has parameter uncertainty, exact cancellation is almost impossible to achieve. When this is the case, such an attempted cancellation will leave an uncompensated unstable mode in the closed-loop system. Even in the case of a stable approximate cancellation the dynamics can change. To see this, consider in Example 5 the pole at -2 to be uncertain (say $-2 \pm \epsilon$, $\epsilon > 0$) and that a zero is exactly located at -2. Let us consider the two cases with the pole at $-2 + \epsilon$ and $-2 - \epsilon$ (Fig. 23).

We note that the modified root loci do not pass through B, B' when $\epsilon \neq 0$, implying that the time-domain performance will be affected.

Example 6 Consider the system shown in Fig. 24*a* where $K \geq 0$ and α and β are unknown constants. To identify K, α, and β, the following information about the system is provided:

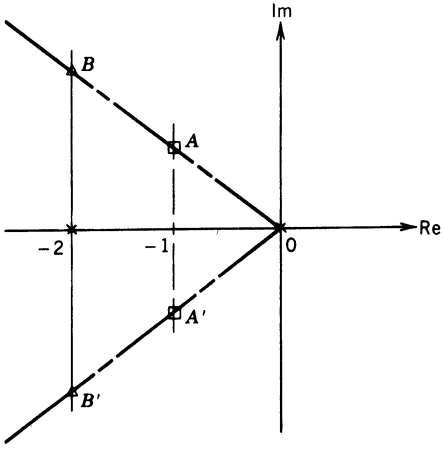


Figure 21 Desired pole locations.

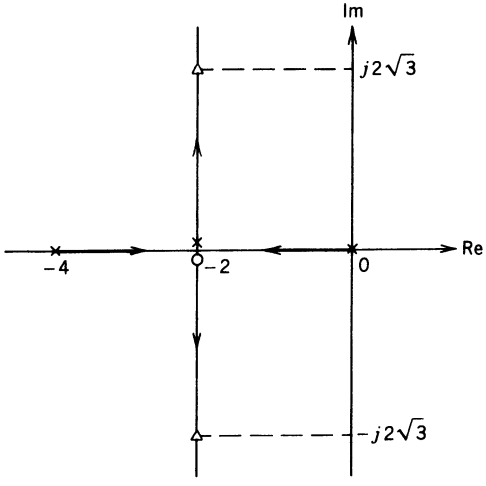


Figure 22 Root loci with pole–zero cancellation.

1. All the poles of the open-loop transfer function are in the closed left-half s-plane.
2. When the closed-loop system is excited by the input $r(t) = tu_s(t)$, the trace of Fig. 24*b* is obtained ($\infty > e_1 > 0$).
3. When the gain K is doubled, the impulse response of Fig. 24*c* is observed.

Determine K, α, and β.

Solution: Since the closed-loop system has a finite steady-state error $e_1 < \infty$ for a ramp input, the system should be type I. Thus we require either α or β to be zero. Let $\alpha = 0$. So it only remains to determine β and K.

Now the root loci for the system can be sketched in the following manner.

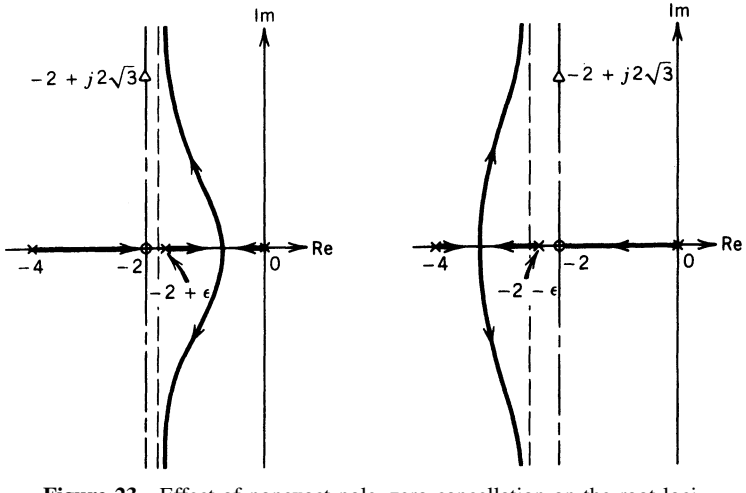
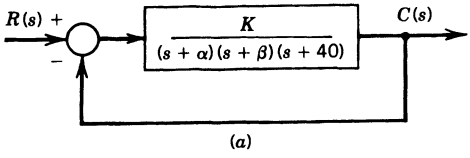
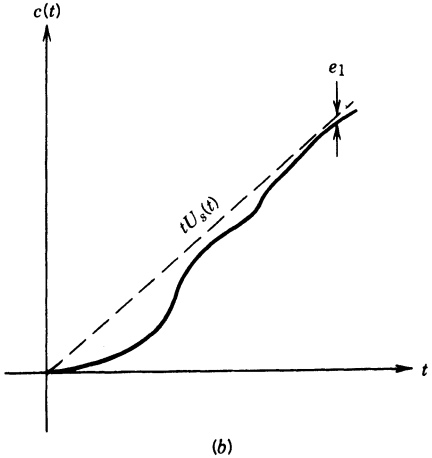


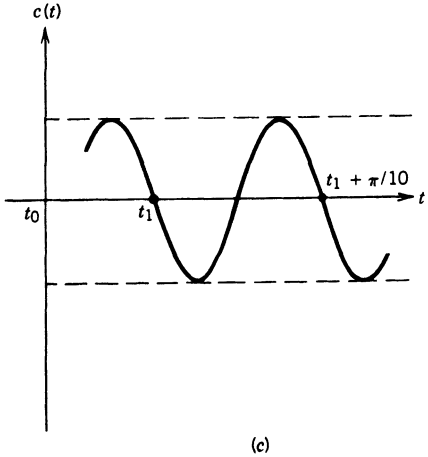
Figure 23 Effect of nonexact pole–zero cancellation on the root loci.



(a)



(b)



(c)

Figure 24 (*a*) System of Example 5; (*b*) response due to a ramp; (*c*) response due to an impulse.

From the root locus it is clear that at a certain gain value the system goes unstable. From Fig. 24*c* we know that when the gain is doubled, the system has two closed-loop eigenvalues at A and A'. From the impulse response trace the frequency of oscillation is

$$\omega = \frac{2\pi}{\pi/10}$$

or

$$\omega = 20 \text{ rad/s}$$

Thus we know that when the gain is doubled, there are two closed-loop poles at $\pm j20$. The corresponding CLCE therefore is

$$P(s) = (s + a)(s + j20)(s - j20) = 0$$

or

$$s^3 + as^2 + 400s + 400a = 0$$

We also know that

$$P(s) = 1 + \frac{2K}{s(s + \beta)(s + 40)} = 0$$

or

$$s^3 + (40 + \beta)s^2 + 40\beta s + 2K = 0$$

By matching coefficients

$$40 + \beta = \alpha$$

$$40\beta = 400$$

$$2K = 400a$$

Therefore $\beta = 10$, $a = 50$, and $K = 10{,}000$. Hence the open-loop transfer function is

$$G(s) = \frac{10{,}000}{s(s + 10)(s + 40)}$$

5.3 Time-Domain Response versus *s*-Domain Pole Locations

Given a transfer function $G(s)$ the pole locations can be found. These pole locations essentially describe the type of time response to be expected. The basic response can be effectively characterized by the impulse response $g(t)$ given by

$$g(t) = \mathcal{L}^{-1}[G(s)]$$

If

$$G(s) = \frac{K\prod_{i=1}^{m}(s + z_i)}{\prod_{j=1}^{n}(s + p_j)} \qquad n \geq m$$

then

$$g(t) = \sum_{j=1}^{n} a_j e^{-p_j t}$$

We note that any real pole contributes an exponential behavior into the time response and a complex-conjugate pair contributes an exponential oscillation. A pure imaginary pair of poles leads to a sustained oscillation. Various components to be expected are shown in Fig. 25.

The role of zeros of the transfer function is to affect the relative weights a_j in the impulse response. For example, if a pole and a zero are close together, the net contribution to the overall response from such a pair will be negligible. If they cancel each other (say $-p_k$ by $-z_j$), then the coefficient associated with the term $e^{-p_k t}$ is zero. This idea can often be used to reduce the order of a dynamic system, that is, remove all pole–zero pairs close to one another. However, care should be exercised not to remove right-half-plane poles and zeros. (See Example 5 of Section 5.2.)

To note the effect of zero locations on the time response consider a second-order oscillatory system with a single zero, that is, consider the transfer function written in the normalized form

$$G(s) = \frac{(s/\alpha\zeta\omega_n) + 1}{(s/\omega_n)^2 + 2\zeta s/\omega_n + 1} = \left(\frac{s}{\alpha\zeta\omega_n} + 1\right) G_0(s)$$

The zero is located at $s = -\alpha\zeta\omega_n$, so if α is large, the zero is far removed from the poles and will have little effect on the response of $G_0(s)$. If $\alpha = 1$, the zero is at the value of the real part of the poles and could be expected to have a substantial influence on the response of $G_0(s)$. The step response curves for $\zeta = 0.5$ and for several values of α are plotted in Fig. 26. We see that the major effect of the zeros is to increase the overshoot M_p with very little influence on the settling time. A plot of M_p versus α is given in Fig. 27. If α is negative, then the zero is in the right-half s-plane. In this case an undershooting phenomenon as shown in Fig. 28 occurs.

In addition, it is useful to know the effect of an extra pole on the standard second-order response $G_0(s)$. In this case consider the transfer function

$$G(s) = \frac{1}{(s/\alpha\zeta\omega_n + 1)} G_0(s)$$

Plots of the step response for this case are shown in Fig. 29 for $\zeta = 0.5$ and for several values of α. In this case the major effect is to increase the rise time, shown in Fig. 30. For a detailed discussion of the effect of a zero and a pole location on a standard second-order response the reader may refer to Ref. 3.

6 POLE LOCATIONS IN THE z-DOMAIN

For discrete-time systems the input–output relation is given by the pulse transfer function. A typical pulse transfer function $G(z)$ is of the form

$$G(z) = \frac{K\prod_{i=1}^{m}(z - \beta_i)}{\prod_{j=1}^{n}(z - p_j)} \qquad n \geq m$$

The poles of the pulse transfer function are p_j, $j = 1, \ldots, n$. As in the case of continuous time, the pole locations determine the stability properties of the system represented by its pulse transfer function. In the z-domain poles have to lie inside the unit circle $|z| = 1$ for

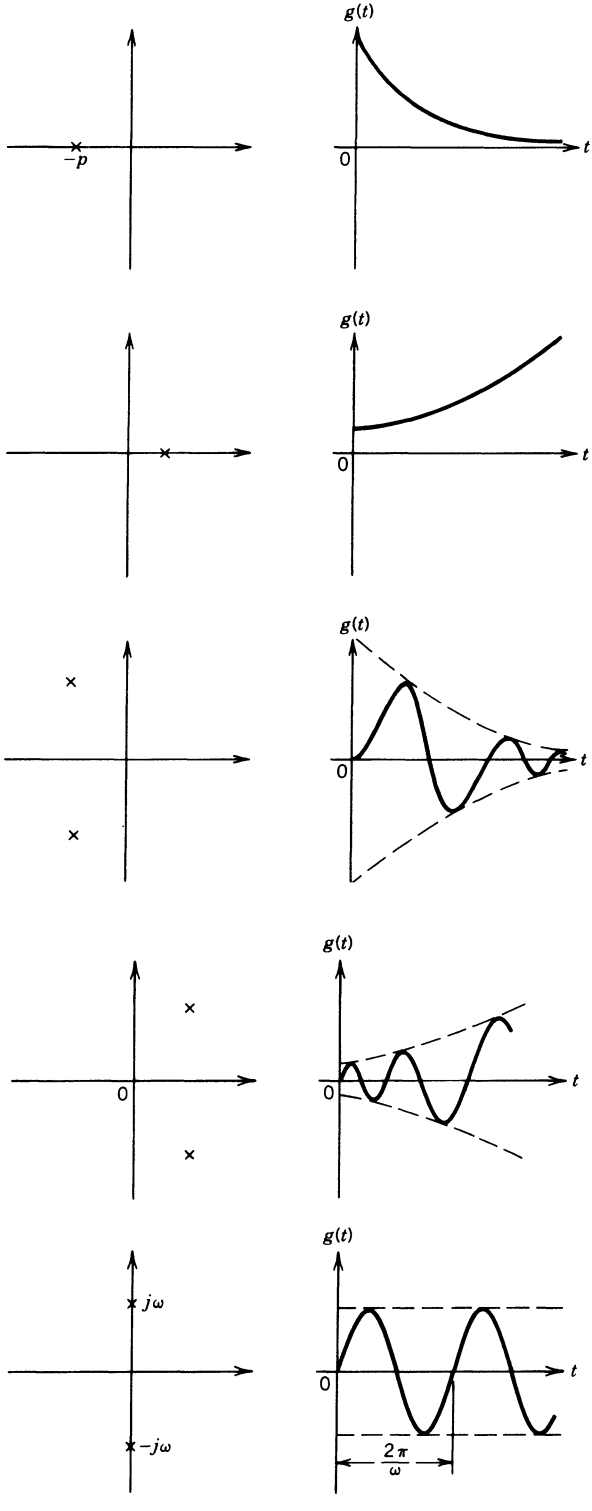


Figure 25 Pole locations and corresponding impulse responses.

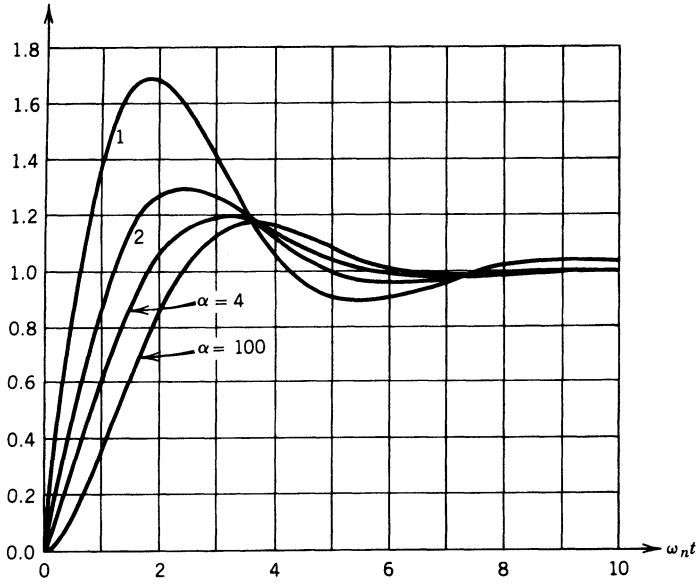


Figure 26 Plots of the step response of a second-order system with an extra zero ($\zeta = 0.5$).

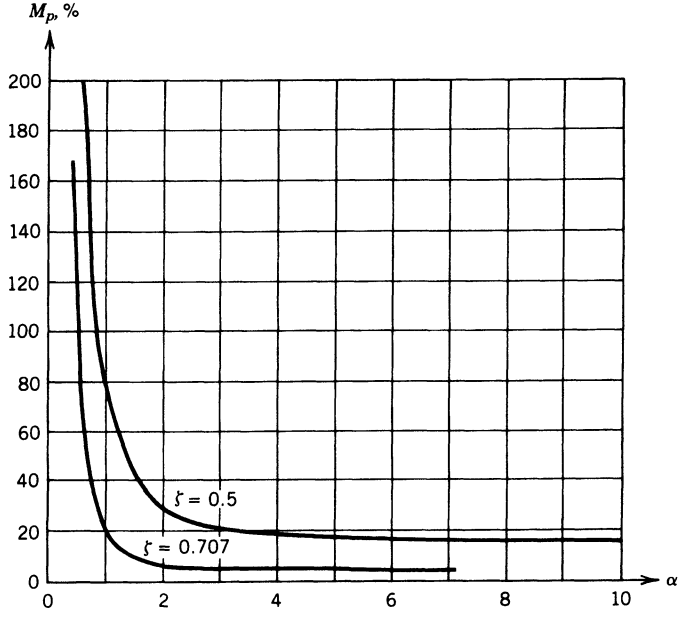


Figure 27 Plot of overshoot M_p as a function of normalized zero location α. At $\alpha = 1$, the real part of the zero equals the real part of the pole.

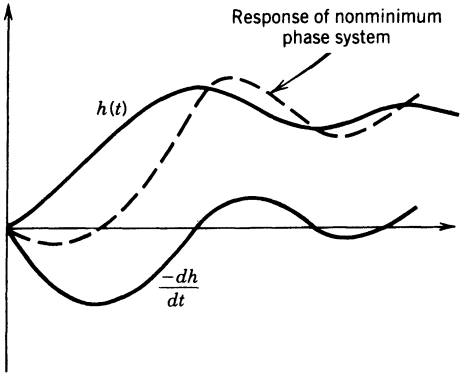


Figure 28 Plot of the response of a second-order system with a right-half-plane zero: a nonminimum-phase system.

asymptotic stability. Thus the open left-half s-plane is equivalent to the interior of the unit circle in the z-domain. The exterior of the unit circle (i.e., $|z| > 1$) represents the unstable region in the z-domain.

6.1 Stability Analysis of Closed-Loop Systems in the z-Domain

Consider a unity negative-feedback system with the closed-loop pulse transfer function

$$\frac{C(z)}{R(z)} = \frac{G(z)}{1 + G(z)} \tag{15}$$

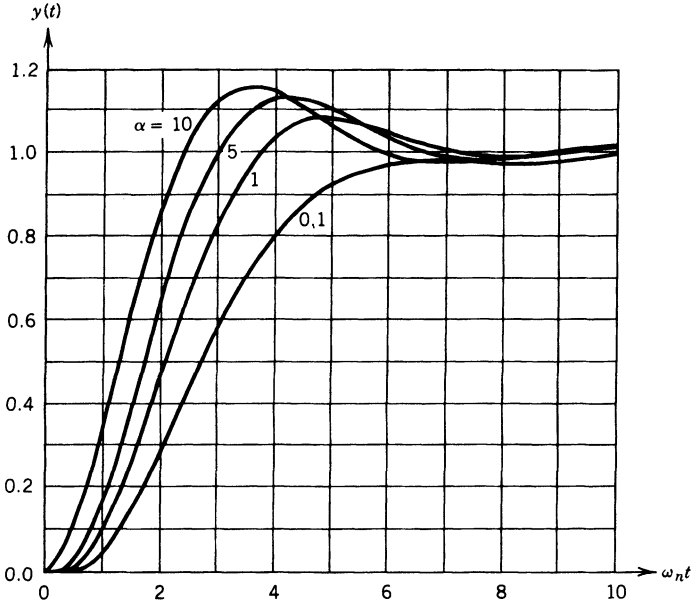


Figure 29 Plot of step response for several third-order systems with $\zeta = 0.5$.

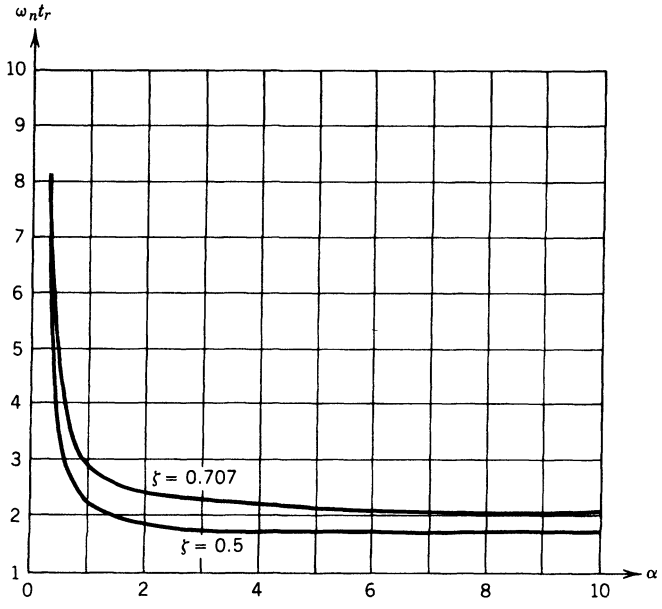


Figure 30 Plot of normalized rise time for several locations of an additional pole.

The stability of the system defined by Eq. (15), as well as of other types of discrete-time control systems, may be determined from the locations of the closed-loop poles in the z-plane or the roots of the closed-loop characteristic equation

$$P(z) = 1 + G(z) = 0$$

as follows:

1. For the system to be stable, the closed-loop poles or the roots of the characteristic equation must lie within the unit circle in the z-domain. Any closed-loop pole outside the unit circle makes the system unstable.
2. If a simple pole lies at $z = 1$ or $z = -1$, then the system becomes marginally stable. Also, the system becomes marginally stable if a single pair of complex-conjugate poles lie on the unit circle in the z-domain. Any multiple closed-loop pole on the unit circle makes the system unstable.
3. Closed-loop zeros do not affect the absolute stability and therefore may be located anywhere in the z-plane. Thus, a linear time-invariant single-input–single-output discrete-time closed-loop system becomes unstable if any closed-loop poles lies outside the unit circle or any multiple closed-loop pole lies on the unit circle in the z-domain.

6.2 Performance Related to Proximity of Closed-Loop Poles to the Unit Circle

In the continuous-time case or in the s-domain the transient performance of a system can be characterized by the s-plane pole locations. Recall that the overshoot is related to the damping ratio ζ.

Damping Ratio ζ

In the s-plane a constant damping ratio may be represented by a radial line from the origin. A constant damping ratio locus (for $0 \leq \zeta \leq 1$) in the z-plane is a logarithmic spiral. Figure 31 shows constant ζ loci in both the s-plane and the z-plane.

If all the poles in the s-plane are specified as having a damping ratio not less than a specified value ζ_1, then the poles must lie to the left of the constant-damping-ratio line in the s-plane (shaded region). In the z-plane, the poles must lie in the region bounded by logarithmic spirals corresponding to $\zeta = \zeta_1$ (shaded region).

Damped Natural Frequency ω_d

The rise time or the speed of response depends on the damped natural frequency ω_d and the damping ratio ζ of the dominant complex-conjugate closed-loop poles. In the s-plane the constant ω_d loci are horizontal lines, while in the z-plane they are radial lines emanating from the origin.

Settling Time t_s

The settling time is determined by the value of attenuation σ of the dominant closed-loop poles $-\sigma \pm j\omega_d$. If the settling time is specified, it is possible to draw a line $\alpha = -\sigma_1$, in the s-plane corresponding to a given settling time. The region to the left of the line $\sigma = -\sigma_1$ in the s-plane corresponds to the interior of a circle with radius $e^{-\sigma_1 T}$ in the z-plane, as shown in Fig. 32.

Remark

To transform s-plane pole locations to the z-domain, the transformation $z = e^{sT}$, where T is the sampling time, is employed.

6.3 Root Locus in the z-Domain

The root locus method for continuous-time systems can be extended to discrete-time systems without modifications, except that the stability boundary is changed from the $j\omega$ axis in the s-plane to the unit circle in the z-plane. The reason for being able to extend the root-locus method is that the characteristic equation for the discrete-time system is of the same form as that for the root loci in the s-plane. For the discrete-time case the CLCE is

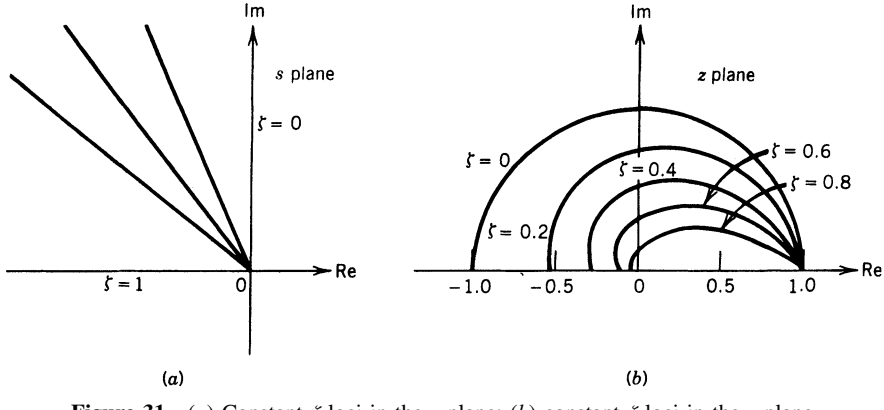


Figure 31 (*a*) Constant ζ loci in the s-plane; (*b*) constant ζ loci in the z-plane.

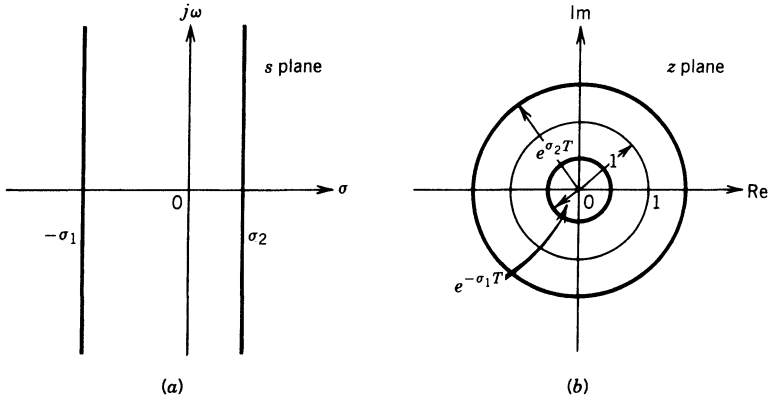


Figure 32 (*a*) Constant attenuation lines in the *s*-plane; (*b*) the corresponding loci in the *z*-plane.

$$1 + G(z) = 0$$

Exactly the same rules as used for the continuous-time case in the *s*-plane can be used for the discrete case too. (See Section 5 for root-loci construction in the *s*-plane.)

Example 7 Consider the closed-loop characteristic equation

$$1 + K\frac{(z + 1)(z - 0.5)}{(z - 1)(z - 0.9)(z + 0.6)} = 0$$

R1: The system has $n = 3$ poles indicating three branches. They start at 1, 0.9, and -0.6 with $K = 0$.

R2: There are two finite zeros ($m = 2$). Hence two of the branches terminate on the zeros -0.9 and 0.5 at $K = \infty$.

R3: One branch ($n - m = 1$) will go to ∞ along an asymptote.

R4: Sections of the root loci on the real line are between 0.9 and 1.0, -1.0 and $-\infty$, and -0.6 and 0.5; with this information the sketch shown in Fig. 33 can be easily obtained. If additional features are needed, the rest of the root-loci construction rules can be applied without change.

7 CONTROLLER DESIGN

In Sections 1–6 some useful tools for designing single-input–single-output systems were given. Once the open-loop system is described, either by its set of poles and zeros or by its frequency response, the root-locus method or frequency response method will indicate whether the feedback system can be given an acceptable transient response by adjustment of the loop gain. The steady-state accuracy can then be determined.

Often good transient performance and good steady-state performance cannot both be achieved simply by adjusting a single parameter such as a loop gain. When this is the case, it is necessary to modify the system dynamics. Either the dynamic properties of some components in the loop need to be altered or additional components need to be inserted into the loop. The process of modifying the system dynamics so as to allow the performance specifications to be met by subsequent loop gain adjustment is known as compensation.

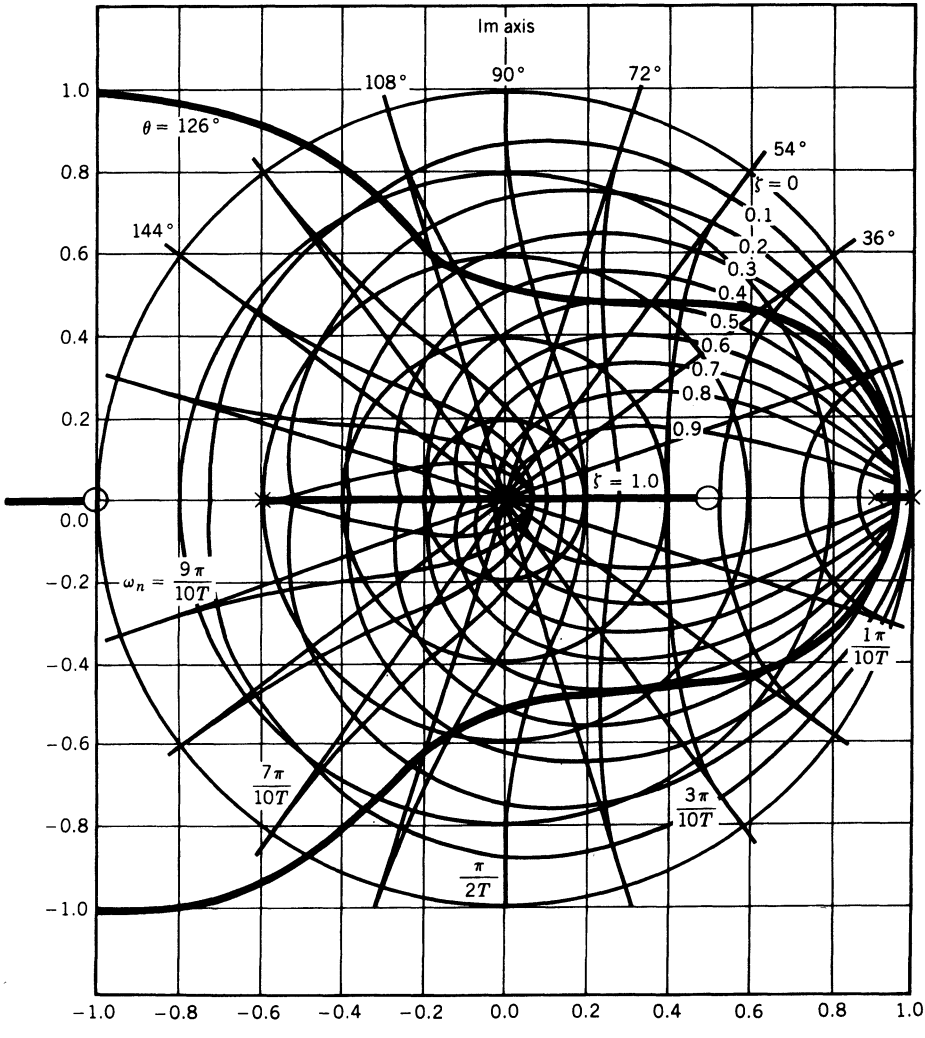


Figure 33 Root loci for Example 7.

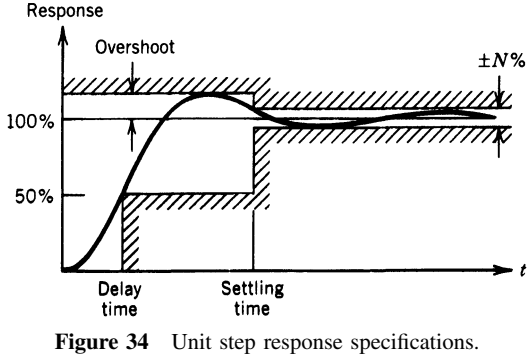


Figure 34 Unit step response specifications.

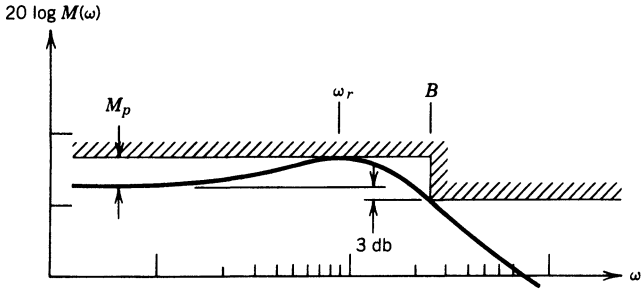


Figure 35 Closed-loop frequency response specifications.

Transient specifications are typically based on a step input response. By specifying the rise time, overshoot, and settling time, the response is confined to within the shaded region of Fig. 34. It is then assumed that a system whose step response satisfies these constraints will have an acceptable transient response to any kind of input.

In the frequency domain the bandwidth and the resonant peak of the closed-loop frequency response are measures roughly corresponding to rise time and overshoot, respectively. Specification of these parameters constrains the magnitude of the closed-loop frequency response to the region shown in Fig. 35. An alternative way of constraining the transient response by frequency-domain criteria is to stipulate the smallest acceptable gain and phase margins.

Often used compensators are the so-called three-term controllers (PID) and lag and lead compensators. These controller or compensator designs are discussed later. They are often done on a trial-and-error basis and can be designed in the *s*-domain or the *z*-domain depending on the type of application. Continuous-time or *s*-domain compensators can often be converted to equivalent *z*-domain compensators by techniques such as pole–zero maps, hold equivalence, and Butterworth pole configurations.[4]

REFERENCES

1. B. C. Kuo, *Automatic Control Systems,* Prentice-Hall, Englewood Cliffs, NJ, 1982.

2. K. Ogata, *Modern Control Engineering,* Prentice-Hall, Englewood Cliffs, NJ, 1970.

3. G. F. Franklin, J. D. Powell, and A. Emami-Naeini, *Feedback Control of Dynamic Systems,* Addison-Wesley, Reading, MA, 1986.

4. G. F. Franklin and J. D. Powell, *Digital Control of Dynamic Systems,* Addison-Wesley, Reading, MA, 1980.

BIBLIOGRAPHY

Bode, H. W., *Network Analysis and Feedback Amplifier Design,* Van Nostrand, New York, 1945.

Chestnut, H., and R. W. Mayer, *Servomechanisms and Regulating Systems Design,* 2nd ed., Vol. 1, Wiley, New York, 1959.

D'Azzo, J. J., and C. H. Houpis, *Linear Control System Analysis and Design,* McGraw-Hill, New York, 1988.

Distefano, J. J., III, A. R. Stubberud, and I. J. Williams, *Feedback and Control Systems* (Schaum's Outline Series), Schaum Publishing, New York, 1967.

Doebelin, E. O., *Control System Principles and Design,* Wiley, New York, 1985.

Dorf, R. C., *Modern Control Systems,* Addison-Wesley, Reading, MA, 1986.

Dransfield, P., *Engineering Systems and Automatic Control,* Prentice-Hall, Englewood Cliffs, NJ, 1968.

Elgerd, O. I., *Control Systems Theory,* McGraw-Hill, New York, 1967.

Eshbach, O. W., and M. Souders (eds.), *Handbook of Engineering Fundamentals,* 3rd ed., Wiley, New York, 1975.

Evans, W. R., *Control-System Dynamics,* McGraw-Hill, New York, 1954.

Eveleigh, V. W., *Introduction to Control Systems Design,* McGraw-Hill, New York, 1972.

Graham, D., and R. C. Lathrop, ''The Synthesis of Optimum Response: Criteria and Standard Forms,'' *AIEE Transactions,* **72** (Pt. II), 273–288, (1953).

Horowitz, I. M., *Synthesis of Feedback Systems,* Academic, New York, 1963.

Houpis, C. H., and G. B. Lamont, *Digital Control Systems: Theory, Hardware, Software,* McGraw-Hill, New York, 1985.

Korn, G. A., and J. V. Wait, *Digital Continuous System Simulation,* Prentice-Hall, Englewood Cliffs, NJ, 1978.

Kuo, B. C., *Digital Control Systems,* Holt, Rinehart and Winston, New York, 1980.

Melsa, J. L., and D. G. Schultz, *Linear Control Systems,* McGraw-Hill, New York, 1969.

Nyquist, H., ''Regeneration Theory,'' *Bell System Technical Journal,* **II**, 126–147, (1932).

Palm, N. J., III, *Modeling, Analysis and Control of Dynamic Systems,* Wiley, New York, 1983.

Phillips, C. L., and H. T. Nagle, Jr., *Digital Control System Analysis and Design,* Prentice-Hall, Englewood Cliffs, NJ, 1984.

Ragazzini, J. R., and G. F. Franklin, *Sampled Data Control Systems,* McGraw-Hill, New York, 1958.

Raven, F. H., *Automatic Control Engineering,* 4th ed., McGraw-Hill, New York, 1987.

Rosenberg, R. C., and D. C. Karnopp, *Introduction to Physical System Dynamics,* McGraw-Hill, New York, 1983.

Shinners, S. M., *Modern Control Systems Theory and Application,* Addison-Wesley, Reading, MA, 1972.

Takahashi, Y., M. J. Rabins, and D. M. Auslander, *Control and Dynamic Systems,* Addison-Wesley, Reading, MA, 1972.

Truxal, J. G., *Automatic Feedback Control Synthesis,* McGraw-Hill, New York, 1955.

Vidyasagar, M., *Nonlinear Systems Analysis,* Prentice Hall, Englewood Cliffs, NJ, 1978.